Journal of Peptide Science
J. Peptide Sci. **6**: 603–611 (2000)

Structural Properties of DNO Investigated with Pyrene Excimer Formation

JÓHANNES REYNISSON[a], LISE VEJBY-CHRISTENSEN[a], ROBERT WILBRANDT[a,1], NIELS HARRIT[b] and ROLF H. BERG[a,*]

[a] Condensed Matter Physics and Chemistry Department, The Danish Polymer Centre, Risø National Laboratory, DK-4000 Roskilde, Denmark
[b] Department of Chemistry, University of Copenhagen, Symbion, Fruebyergvej 3, DK-2100 Copenhagen, Denmark

Received 7 June 2000
Accepted 12 June 2000

Abstract: Four diamino acid-N^{α}-substituted oligopeptide (DNO) oligomers substituted with pyrenyl as photophysical probes were synthesized. The excimer formation and ground-state association of the pyrenyl groups were investigated by means of absorption and steady-state fluorescence spectroscopy together with time-resolved fluorescence techniques. The photophysical parameters obtained from the different derivatives reflect the secondary structural properties of the DNO backbones. Copyright © 2000 European Peptide Society and John Wiley & Sons, Ltd.

Keywords: DNO; pyrene; absorption; fluorescence; excimer

INTRODUCTION

Peptides are ideally suited for the design and synthesis of novel molecules and materials with potentially interesting structures and functions [1–3]. Recently, a novel class of peptides containing azobenzene chromophores was investigated as materials for optical storage of information [4–6]. By analogy with the design of peptide nucleic acids (PNA) [7–9], these so-called diamino acid-N^{α}-substituted oligopeptides (DNOs) were designed with a molecular geometry similar to that of DNA so as to impose orientational order on the chromophores. The DNO backbone is made up of diamino acids, e.g. ornithine (Orn) units (Figure 1) dimerized or oligomerized through the δ-amino groups and with the chromophores attached to the α-amino groups by carbonyl linkers.

It has not been possible to obtain direct structural information about DNOs via X-ray crystallography or NMR spectroscopy since these compounds are slightly soluble in common solvents and very hard to crystallize [5,6]. Among alternative means,

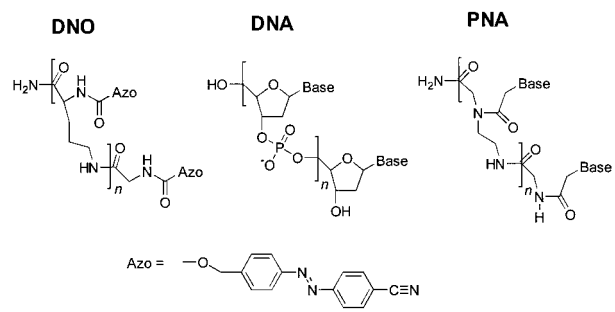

Figure 1 Chemical structures of Orn-based DNO substituted with azobenzene chromophores, DNA and PNA.

Abbreviations: Dab, diaminobutyric acid; Dap, diaminopropionic acid; DNO, diamino acid-N^{α}-substituted oligopeptide; excimer, excited dimer; HPLC, high performance liquid chromatography; MALDI-TOF, matrix assisted laser desorption ionization-time of flight mass spectroscopy.

* Correspondence to: Condensed Matter Physics and Chemistry Department, The Danish Polymer Centre, Risø National Laboratory, DK-4000 Roskilde, Denmark.
[1] Present address: Bornholms Amtsgymnasium, Søborgstræde 2, 3700 Rønne, Denmark.

photophysical probes have been used extensively in order to investigate the structure and dynamics of molecules in dilute solution [10]. In the present paper, the structural properties of DNO investigated with pyrene excimer (excited dimer) formation are reported. Excimer formation of two pyrene moieties is one of the more widely used photophysical probes [11]. The pyrene excited singlet state has the interesting property of efficient excimer formation with its ground state counterpart, as well as a high fluorescence quantum yield and a long lifetime ($\phi_{fl} = 0.72$ [12], $\tau_{fl} = 190$ ns in polar solvents [13]). The excimer is largely deactivated by emission, which occurs at lower energy ($\lambda \sim 480$ nm) than the fluorescence of the monomer singlet state ($\lambda \sim 380$ nm). These properties make a pyrene pair an excellent photophysical probe. The first obvious consequence of pyrene chromophores being linked to the same molecule is the greatly enhanced local concentration of the chromophores allowing excited state complex formation at very low concentrations. The extent of excimer formation is limited by the probability for a molecule containing two pyrenyls to reach, within the lifetime of the excited singlet state, a conformation suitable for excimer formation [14]. The interchromophore face-to-face distance of excimers has been estimated to be ca. 3–3.5 Å in diaryl-substituted polypeptides [15]. However, due to molecular fluctuation at room temperature and the attractive forces of the excimer described here, the critical distance of excimer formation is ca. 4.5 Å for pyrenyl substituents in peptides [15].

Winnik has described very useful experimental criteria for the detection of pyrene ground-state association and excimer formation in supramolecular systems utilizing absorption and fluorescence spectroscopic techniques [11]. The ^1L_a absorption band has a distinct vibronic structure, which is partly smeared out when association between two pyrene moieties occurs in the ground state. Thus, the peak-to-valley ratio of the (0,0) transition of the ^1L_a band and its adjacent minimum, respectively, is a convenient way of measuring this loss of resolution (see Results section for further details) [11]. A small bathochromic shift in the (0,0) transition (^1L_a) at 341–332 nm of the excimer fluorescence excitation spectrum relative to that of the monomer [$\Delta\lambda = \lambda_{max}$ (excimer) $- \lambda_{max}$ (pyrene)] is also indicative of a ground-state association [11]. In systems where association occurs, $\Delta\lambda$ takes a positive value from 1 to 4 nm [11].

For this work four DNOs were prepared, each substituted with a pair of pyrenyl groups (**DNO-1**, **DNO-2**, **DNO-3** and **DNO-4**, Figure 2). In **DNO-1**, 2,3-diaminopropionic acid (Dap) forms a dipeptide with glycine (Gly) via the β-amino group. Thus, a total of four bonds connect the α-carbons. The pyrenyl moieties are attached via methylcarbonyl links to the α-nitrogens. Similarly, **DNO-2** and **DNO-3** are based on 2,4-diaminobutyric acid (Dab) and Orn, respectively, rendering five and six bonds between the α-carbonyls. The **DNO-4** backbone is a tripeptide that constitutes two Orn and one Gly, a total of 12 bonds connecting the terminal α-carbonyls. (1-Pyrenyl)glycine (**1**) was prepared as a reference. The absorption, fluorescence excitation and emission spectra of the derivatives have been measured as well as the lifetimes of the fluorescence emissions. The data are analysed for information on the DNO backbone's structure and dynamics based on the experimental criteria defined by Winnik [11] and by comparison with forcefield calculations.

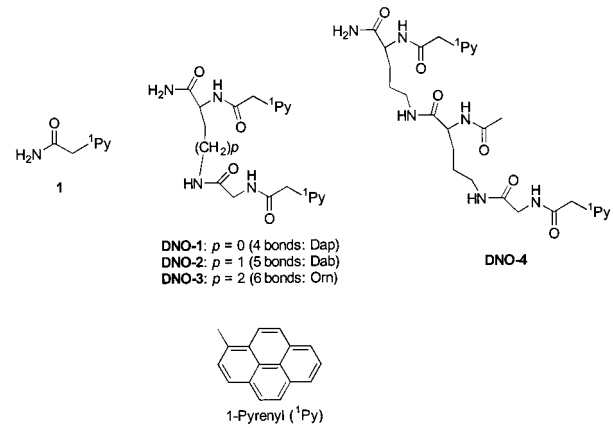

Figure 2 Chemical structures of the DNOs used in this study.

MATERIALS AND METHODS

The DNOs were synthesized by stepwise Merrifield synthesis [16,17] using a synthetic protocol similar to the one previously reported for azobenzene-substituted DNO [4] except that (1-pyrenyl)acetic acid was used as the side-chain monomer. The DNOs were purified by semi-preparative HPLC and were shown to have the expected molecular masses by MALDI-TOF mass spectrometry.

The absorption spectra were measured on a Perkin–Elmer Lambda 5 UV/VIS Spectrophotometer using 1×1 cm optical quartz cells. Solutions

($\sim 1 \times 10^{-5}$ M in methanol) were prepared in order to obtain the fluorescence excitation and emission spectra and lifetimes. Methanol (HPLC-quality) was used as received. It showed no fluorescence at the excitation wavelengths employed.

For steady-state fluorescence emission and excitation spectra an FS900, Edinburgh Analytical Instrument luminescence spectrometer was used. A highly concentrated (ca. 5 g/L) solution of Rhodamine B in glycerol was used as a quantum counter in order to correct the excitation spectra. Raman scatter did not interfere with any of the fluorescence spectra shown.

The fluorescent lifetimes were measured on a time-correlated single-photon-counting (SPC) apparatus (FL900, Edinburgh Analytical Instruments) using a nanosecond flash-lamp filled with either nitrogen or hydrogen. The excitation wavelength was set at 337 nm, thus using the nitrogen line at this wavelength when measuring lifetimes longer than 10 ns. For lifetimes shorter than 10 ns hydrogen gas was used. Emission was monitored at 378 and 466 nm. The detector photo-multiplier tube was a Hamamatsu R1527. A Ludox dispersion was used to obtain the instrument response function. Fluorescence decay curve analysis was performed by reconvolution of the instrument response function with an assumed decay law. The decay parameters were determined by a least-squares fitting routine, the quality of which was evaluated by the reduced χ^2 values, as well as by the randomness of the weighted residuals. Both steady-state and time-resolved fluorescence experiments were performed in the normal 90° configuration. All samples were purged with argon prior to fluorescence emission measurements.

The program HyperChem 4.0 [18] was used for geometry optimization with the MM+ force-field package.

RESULTS

Absorption

The absorption spectrum of the monomer **1** is shown in Figure 3. The absorption spectra of **DNO 1–4**, each including two pyrene chromophores, are qualitatively identical except for the observation of broadening of the vibronic bands and a slight red shift of ca. 1 nm for the band at 341 nm. A convenient relative measure for this loss in resolution can be extracted from the ratio P_A (Figure 3) between the absorption intensity of the most intense band (341 nm, (0,0) transition in ^1L_a band) and that of the adjacent minimum at the shorter wavelength [11]. This ratio is usually smaller than 3.0 when a ground-state association occurs between 1-substituted pyrenyl groups [11].

The P_A values were determined for all the derivatives and the results are given in Table 1. Markedly higher values were found for **DNO 1–4** relative to **1**. This means that ground-state association occurs in all the doubly-substituted derivatives. The numbers show, that the phenomenon is more dominant in **DNO-1** while successively less interaction is observed between the ground-state pyrenyls in **DNO-2**, **DNO-3** and **DNO-4**.

Steady-state Emission Spectra

The fluorescence spectra obtained are depicted in Figure 4. All of the DNO derivatives with two pyrenyl moieties exhibit emission at 466 nm, albeit the relative intensity of the **DNO-2** is very small. This emission originates from intramolecular pyrenyl excimers, because negligible fluorescence was observed at 466 nm from a solution of **1** at the same pyrenyl concentration. The excimer emission maximum is found at the same wavelength for all the derivatives, which implies that the same excimer species is present.

The relative efficiency of excimer fluorescence is expressed by the ratio I_E/I_M of intensities measured at the maxima of excimer ($I_E = 466$ nm) and monomer ($I_M = 378$ nm) emissions, respectively [11]. I_E/I_M was determined for all the derivatives. The values are shown in Table 1. It is apparent that **DNO-1** has the most intensive excimer emission

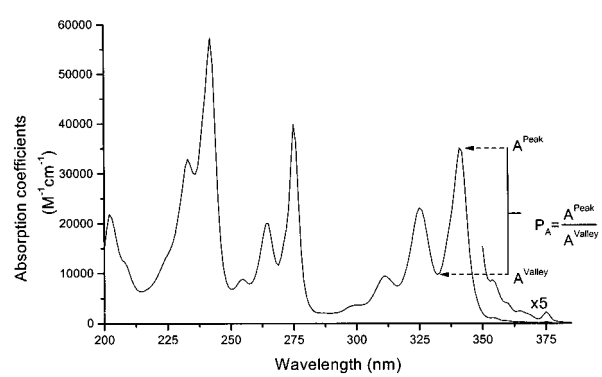

Figure 3 Absorption spectrum of monomer **1** in methanol at room temperature. As indicated, absorbance values of the ^1L_a (0,0) band at 341 nm and the adjacent valley at 332 nm are used to determine P_A.

Table 1 Absorption, Emission, Excitation and Time-resolved Fluorescence Data for Monomer **1** and **DNO 1–4**

	Absorption	Emission	Excitation		Time-resolved fluorescence (ns)		
	P_A^b	I_E/I_M^b	P_M^b	P_E^b	τ_M^c	τ_E^b	τ_F^d
1	3.6	x	3.4	x	153[b]	x	x
DNO-1	2.3	15.8	3.0	2.4	2.1	42.4	0[a]
DNO-2	2.4	0.2	2.6	1.7	62.4[b]	36.5	0[a]
DNO-3	2.8	3.2	2.3	2.4	3.0	34.8	3.5
DNO-4	2.9	10.3	2.3	2.2	3.8	41.3	4.5

I_E/I_M is the ratio of the monomer and excimer steady-state emissions. P_A is the peak-to-valley ratio for the absorption spectra. P_M and P_E are the peak-to-valley ratios for the monomer and excimer excitation spectra, respectively (see Figure 5). The time-resolved values are the monomer emission lifetimes (τ_M), excimer lifetimes emission (τ_E) and the formation time of the excimer (τ_F). x, no excimer emission observed.
[a] Time resolution not adequate.
[b] Estimated error $\pm 5\%$.
[c] Estimated error $\pm 10\%$.
[d] Estimated error $\pm 15\%$.

relative to monomer fluorescence, followed by **DNO-4**. The ratio drops further by a factor of three when proceeding to **DNO-3**, while hardly any excimer emission is observed from the **DNO-2** derivative.

Excitation Spectra

The monomer and excimer emission excitation spectra for **DNO-1** are depicted in Figure 5. Formation of excimers by excitation of pre-associated pyrenyls in the DNO-series can be revealed by comparing the adjacent peak-to-valley ratio for the (0,0) transition in the ^1L_a band (341–342 nm) of the excitation spectra recorded at the monomer ($P_M = I_M^{Peak}/I_M^{Valley}$) and the excimer ($P_E = I_E^{Peak}/I_E^{Valley}$, see Figure 5) emissions maxima [11]. The monomer **1** does not have an opportunity to form a ground-state complex due to its low concentration (1×10^{-5} M) [19], hence its relatively large P_M value. In situations where a larger fraction of the emitting excimers have been formed by excitation of a pre-associated pair of pyrenyls, P_E is smaller than P_M [11]. As can be seen from Table 1, this phenomenon is observed in the case of **DNO-1** and **DNO-2**. Pre-association also occurs for **DNO-3** and **DNO-4**, since the P_M and P_E values (2.2–2.3) both are smaller than that found for the monomer **1** ($P_M = 3.4$). However, the same values are found for P_M and P_E so the interaction between the pyrenyls has no consequence for the relative distribution between monomer and excimer emission.

A small red shift is observed when going from the wavelength maximum for the (0,0) transition in the ^1L_a band of the excimer excitation spectrum to that of the monomer excitation. The shift is 1 nm for **DNO-3** and **DNO-4** and 2 nm for the **DNO-1** and **DNO-2** derivatives. This increase supports the conclusion based on the peak-to-valley criteria, i.e. the **DNO-1** and **DNO-2** derivatives exhibit more extensive ground-state association than **DNO-3** and **DNO-4**.

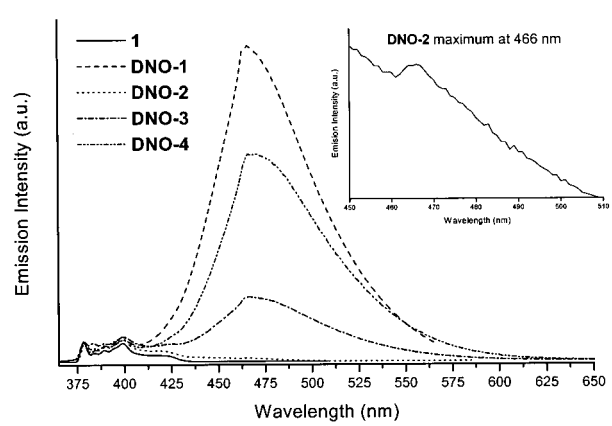

Figure 4 Steady-state fluorescence spectra in methanol at room temperature ($\sim 1 \times 10^{-5}$ M). Maxima of the monomer emission are located at 378 (I_M) and 399 nm. The spectra are normalized in the monomer band at 378 nm. Excimer fluorescence (I_E) shows a maximum at 466 nm in each case. The inset depicts a magnification of the **DNO-2** excimer fluorescence band.

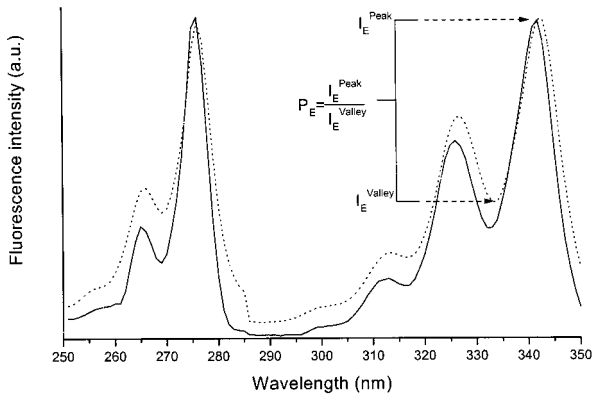

Figure 5 Normalized excitation spectra of **DNO-1** in methanol at room temperature. Emission is monitored at 378 nm (monomer, full line) and 466 nm (excimer, dotted line), respectively. The loss in resolution is reflected in the P_M (monomer) and P_E (excimer) values determined from the ratio of the intensities at 341–342 nm and its adjacent valley. Only determination of the P_E value is illustrated.

Time-resolved Fluorescence

The lifetime of the observed fluorescence was measured at the monomer (378 nm, τ_M) and the excimer (466 nm, τ_E) emission wavelengths. The results are shown in Table 1. The decay of the **DNO-3** excimer emission is displayed in Figure 6. Single exponential decays were observed for all monomer and excimer emissions. Thus, it can be concluded that the excited state in each case is dominated by a single conformation.

Monomer **1** has a long lifetime, close to the lifetime of unsubstituted pyrene (190 ns in ethanol [13]). The lifetime of the monomer response at 378 nm of **DNO-1**, **DNO-3** and **DNO-4** are much shorter due to excimer formation, which deactivates the pyrene singlet state. Almost no competitive excimer formation is observed for **DNO-2**.

It was possible to monitor formation of the excimers of the **DNO-3** and **DNO-4** dimers as shown in Figure 7. It was not possible to observe the formation of the **DNO-1** and **DNO-2** excimers, which must fall within the picosecond regime. The time profiles of the **DNO-3** and **DNO-4** derivatives were fitted to Equation (1) [20]:

$$I_E(t) = A(1 - \exp(-t/\tau_F)). \quad (1)$$

The formation times (τ_F) thus obtained are given in Table 1. The **DNO-3** derivative exhibits a faster excimer formation rate than its **DNO-4** counterpart. The monomer lifetimes (τ_M) and excimer rise times (τ_F) for the **DNO-3** and **DNO-4** derivatives correlate well, connecting the deactivation of the pyrene singlet state and the formation of the excited dimer.

Force-field Calculations

The structures were optimized from the classical B-DNA geometry with the MM+ force-field package. The average distance between pyrenyl moieties obtained for the DNO derivatives is 4.0 ± 0.1 Å, which is within the critical distance of excimer formation predicted to be ca. 4.5 Å for pyrenyl-substituted peptides [15]. The angles between the molecular long axis of the pyrenyl moieties were determined as $19.1 \pm 0.2°$ for the **DNO-2**, **DNO-3** and **DNO-4** derivatives. However, the **DNO-1** exhibits an angle of 10.0°. The molecular mechanics results have to be interpreted carefully, since solvent and electronic effects are omitted. In particular, hydrogen bonds

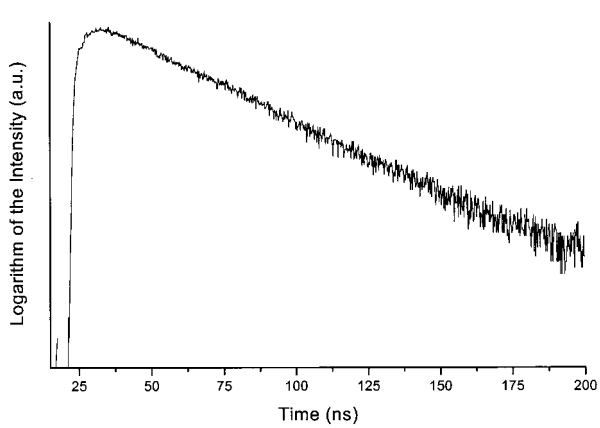

Figure 6 Emission decay curve of **DNO-3** excimer emission, monitored at 466 nm in methanol at room temperature.

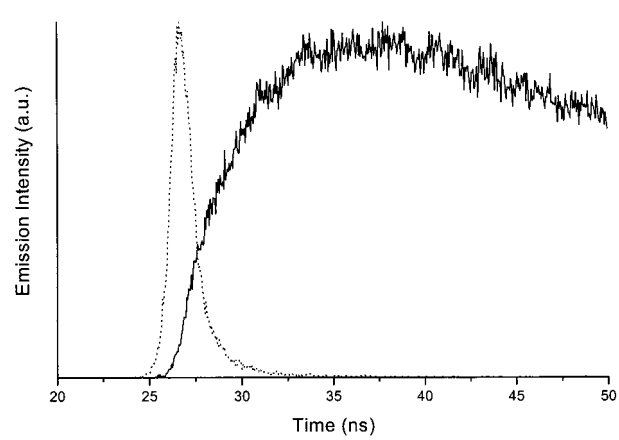

Figure 7 The grow-in of the excimer fluorescence for **DNO-4** measured in methanol at room temperature.

cannot be simulated within the MM+ package. Since these non-covalent interactions cannot be effectively reproduced, only qualitative conclusions should be drawn from these calculations.

The excimer state has been described theoretically by configurational mixing of exciton–resonance states and charge resonance states [21,22]. The optimal geometry of the pyrenyls is the parallel arrangement of the molecular long axes in the excimer state. Both the exciton and resonance interactions favour a sandwich-like structure since it yields the smallest distance between the molecular centres [21]. These geometrical requirements for excimer formation are met reasonably well by the DNO-geometries predicted by the MM+ package.

DISCUSSION

It has been observed that the intensity of the excimer emission in pyrene-labelled polypeptides is dependent on the chirality of the 1-pyrenylalanine employed in their synthesis [23]. Circular polarized fluorescence spectra (CPF), of pyrene-labelled polypeptides, show negative and positive dissymmetries in the pyrene excimer emission wavelength range [24]. Dissymmetric CPF spectra are diagnostic of the presence of the more than one emissive species [25]. Egusa *et al.* [23,26] attributed the dissymmetry observed in the CPF spectra of pyrene-labelled polyalanines to the presence of two kinds of excimer species: a non-polar excimer ($\lambda_E = 460$ nm) of well-defined geometry and a polar excimer emitting at longer wavelengths ($\lambda_E = 520$ nm), which may exist in a variety of configurations and where the interchromophoric distance is longer than for the non-polar excimer.

In the present study, the pyrene excimer emission maximum is invariably found at 466 nm for the **DNO** series, which means that the hypothetical non-polar excimer species are predominant. Furthermore, in all lifetime measurements – monomer or excimer – a strictly monoexponential decay was observed and only insignificant variation was observed in the excimer lifetime (τ_E, Table 1). These findings support the existence of a single equilibrium excimer geometry common to all the molecular systems.

The structural differences among the **DNO** derivatives rely mainly on the length of the backbone connecting the amide units bearing the pyrenyl substituents (Figure 2). **DNO-1**, **DNO-2** and **DNO-3** are DNO-dimers having a linking chain of four, five and six bonds, respectively, between the α-carbonyls of the dipeptide. **DNO-4** is a tripeptide with a total of 12 bonds in the linking chain including the intermediate amide group.

The increasing chain length in the series **DNO 1–4** is parallel to the observed increase in the P_A parameter (Table 1), being derived from the absorption spectra. A smaller P_A value, as observed for **DNO-1**, means stronger interaction between the ground-state pyrenyls. Still, they are not completely independent even in **DNO-4**, since the P_A value remains markedly lower than that for the free monomer **1**. From the absorption data alone it cannot be concluded, whether the increased decoupling in the series **DNO 1–4** relates to higher flexibility of the longer chains or if a generally rigid configuration is increasingly unfavourable for interaction between the pyrenyls.

However, the ratio between the relative fluorescence intensities originating from excimer and excited monomer (I_E/I_M, Table 1) decreases dramatically when going from **DNO-1** ($I_E/I_M = 15.8$) to **DNO-2** ($I_E/I_M = 0.2$). Apparently, the dominating ground-state configuration of **DNO-2** represents a very unfavourable geometry for excimer formation from ground-state associated pyrenyls. Furthermore, the configuration is locked so that any configurational diffusion is prohibited. Since the **DNO-1** backbone is shorter than that of **DNO-2**, restricted mobility of the pyrenyls must also be expected in **DNO-1**. In this case, however, the dominating ground-state configuration is very favourable for excimer formation as reflected in the high I_E/I_M value. An increase in relative excimer intensity is observed when proceeding from **DNO-2** to **DNO-3** ($I_E/I_M = 3.2$) and even further in the case of **DNO-4** ($I_E/I_M = 10.3$). As shall be seen, this trend is due to increased flexibility of the linkers, thus permitting the pyrenyls to diffuse together during the excited state lifetime. Thus, for **DNO-4** an efficient excimer formation is observed in spite of the relatively weak interaction between the pyrenyls in the ground state.

It is important to distinguish between the peak-to-valley ratios obtained from absorption (P_A) and excitation spectra (P_M and P_E), respectively (see Table 1). While an absorption spectrum reflects the situation in the whole molecular population, an excitation spectrum only concerns the ground-state molecules leading to the emission monitored.

For both **DNO-1** and **DNO-2**, P_M is greater than P_E, which means that the pyrenyls leading to monomer fluorescence are less associated than

those forming excimers. In the case of **DNO-3** and **DNO-4** the P_M values are smaller (2.3) and in level with the P_E values (2.2–2.4).

Therefore, the monomer and excimer fluorescence originate from excitation of the same conformational population. This is characterized by a relatively strong association between the pyrenyls since the P_M and P_E values (2.3–2.4) are substantially smaller than the $P_M = 3.4$ value for the monomer **1**. However, the mutual orientation of the pyrenyls is not favourable for excimer formation. Following excitation, the relative intensities of excimer and monomer emissions from **DNO-3** and **DNO-4** are determined by the competitive processes of monomer radiative deactivation and conformational diffusion towards a pre-excimer geometry. As can be seen from the I_E/I_M ratios, the last process is most efficient in the case of **DNO-4** thereby demonstrating a greater flexibility of the longer **DNO-4** linker in spite of the intermediate peptide bond.

The peak-to-valley ratio derived from the excimer excitation spectra vary insignificantly among the **DNO-1**, **DNO-3** and **DNO-4** derivatives ($P_E = 2.2$–2.4). Only **DNO-2** stands out with a markedly smaller value ($P_E = 1.7$). As mentioned above, this result only concerns the molecules that actually display excimer fluorescence, which is a minute fraction in the case of **DNO-2**. These, on the other hand, already interact strongly in the ground state. This finding elaborates the model derived above. There appears to be (at least) two ground-state populations of **DNO-2** molecules which are *not* interconvertible on a timescale shorter than the lifetime of the excited singlet state. In the major population, the configuration is fixed very unfavourably for excimer formation and monomer fluorescence dominates. In a small fraction, strong pre-association and 'pre-excimer' geometry leads to excimer formation and emission.

In the force-field calculations, an angle of 10.0° was found between the long axis of the pyrenyl moieties of **DNO-1** while ca. 20° displacement was predicted for **DNO-2** (and **DNO-3/4)**. Since a coaxial configuration is considered the optimum geometry for excimer formation [21,22], this result — in combination with the rigid framework — is consistent with the vastly more efficient excimer formation (I_E/I_M value, Table 1) found for **DNO-1** relative to **DNO-2**.

The time-resolved measurements give further information. The fluorescence lifetime of the monomer **1** is 153 ns (Table 1). This is shortened by a factor of 50 or more in the molecules **DNO-1**, **DNO-3** and **DNO-4** due to the competitive excimer formation. In the case of **DNO-2** a much longer lifetime is observed in agreement with the model described above, since the majority of excited singlet pyrenyls are prohibited from deactivation by excimer formation.

In the case of **DNO-3** and **DNO-4** a grow-in of the excimer fluorescence could be observed. As can be seen from Table 1, a good agreement is observed in each case between the excimer formation time (τ_F) and monomer singlet lifetime (τ_M). This means that excimer formation is the dominant deactivation path for the excited monomer, the rate being determined by conformational diffusion.

Interesting is the fact, that no grow-in could be observed in the case of **DNO-1** and **DNO-2** in spite of the either very long (**DNO-2**) or still observable (**DNO-1**) monomer lifetimes. These observations are fully compatible with previous conclusions. A major population of **DNO-1** molecules holds a configuration with strong interaction among the pyrenyls and a mutual orientation optimal for excimer formation (pre-association). When excited, these molecules form excimers on a sub-nanosecond timescale. A minor fraction of the **DNO-1** molecules is not perfectly in line with the excimer configuration and the excited pyrenyl lives long enough ($\tau_M = 2.1$ ns) in order to fluoresce a little before it is deactivated by (mainly) excimer formation. The relative contribution from these molecules to the excimer emission intensity is too small in order to manifest itself in the on-set profile.

On the contrary, the majority of the **DNO-2** molecules are fixed in a configuration prohibitive for excimer formation and fluoresce as the monomer with long lifetime. A minute fraction is held in a strongly interacting, pre-excimer configuration, which generates the excimer with a sub-nanosecond rate upon excitation.

When pyrene is used as a conformational probe, it is customary to distinguish between 'dynamic excimers' and 'static excimers' [11]. The first term refers to Birks' original picture for excimer formation as a result of a diffusional encounter between individual monomers, one of them in the excited singlet state and the other in the ground state. This process usually occurs on a nanosecond time-scale. When the excimer is formed by direct excitation of a ground-state dimer, it is called 'static' even though its formation should be observable with sub-nanosecond resolution [11]. In the DNO derivatives studied in this work, however, ground-state interaction is observed to a varying degree as deduced from

the absorption and excitation spectra of all four derivatives. But static excimer formation is only observed in the case of **DNO-1** and to a small extent for **DNO-2**. Some examples have been reported in the literature of strongly interacting pyrene moieties showing no excimer emission [23,27,28]. Oishi *et al.* [29] have reported on the photophysical properties of a peptide carrying two pyrene residues which formed a sandwich-type close pair in the ground state as evidenced by CD spectroscopy. Still, no excimer emission was observed. It is argued that formation of a strictly fixed sandwich type ground-state dimer hinders the formation of an excimer [29]. These reports demonstrate that a strong interaction in the ground state, manifesting itself in absorption spectroscopy or circular dichroism, does not necessarily imply efficient excimer emission.

The high affinity of the **DNO-1** and **DNO-2** derivatives to form ground-state complexes and the restricted conformational freedom in the excited state are imposed onto the pyrene moieties by the DNO backbone. In contrast, the longer linkers of **DNO-3** and **DNO-4** are less rigid, thereby allowing for dynamic excimer formation from a less interacting pair of ground-state pyrenyls. Among these two, the **DNO-4** linker provides the greatest configurational freedom since excimer formation is efficient (high I_E/I_M) in spite of weak ground-state interaction (high P_A). This conclusion is also evidenced by the relatively longer monomer fluorescence lifetime (τ_M), excimer formation time (τ_F) and excimer lifetime (τ_E) for **DNO-4** compared to **DNO-3**.

It has been observed that protic solvents, which are able to form hydrogen bonds, reduce excimer formation in pyrene-labelled polypeptides [30]. Hydrogen bond forming solvents shift the equilibrium towards random coil conformation, which is unfavourable for excimer formation [30]. The extensive excimer formation of the **DNO-1**, **DNO-2** and **DNO-3** derivatives and the clear ground-state association of the **DNO-2** derivative in methanol reveals that the DNO backbone is not particularly susceptible to random coiling even in protic solvents.

It has been reported that helical polypeptide chains are rigid enough to support side-chain groups, including such large chromophores as pyrenyl groups, in a specific spatial arrangement [15]. In agreement, the experimental results reported herein also point towards the decisive role played by the specifically designed secondary helical structure of the DNO backbone [4].

CONCLUSIONS

The pyrenyls of all of the doubly-substituted DNO derivatives are associated to some extent in the ground state or are in the relative vicinity of each other when excited. This proximity is imposed on them by the DNO backbone. These results exclude the possibility of a random coiled configuration of the polypeptide. However, as deduced from the time-resolved measurements, each derivative displays individual dynamic properties, and ground-state interaction occurs without necessarily leading to static excimer formation upon excitation:

1. For **DNO-1** the situation is relatively straightforward. In the major ground-state population pre-association prevails, and 'static' excimers are formed with great efficiency. In a minor ground-state population, however, deactivation via the excimer occurs dynamically by configurational diffusion.
2. As to **DNO-2**, the major ground-state configuration is strongly unfavourable for excimer formation. Apparently, the pyrenyls are sufficiently close to each other, but the molecular axis make an angle. The rigid backbone prevents reorientation and monomer emission dominates. However, in a minute fraction of the ground-state molecules pre-association is tight and static excimer formation occurs.
3. For **DNO-3** and **DNO-4**, the ground-state interaction occurs in a mutual orientation of the pyrenyls, that does not allow static excimer formation. The backbones are flexible, however, and excimer formation occurs with a rate determined by conformational diffusion. In terms of efficiency, the longer **DNO-4** linker proves more efficient (or less prohibitive) than the shorter **DNO-3** linker in spite of the amide group being part of the **DNO-4** linker.

Acknowledgements

The authors thank Ms. Anne Bønke Nielsen for skilled technical assistance. This work was supported by a PhD grant from the Danish Research Academy (J.R.).

REFERENCES

1. Voyer N. *The Development of Peptide Nanostructures*. *Topics in Current Chemistry*. Springer Verlag: Berlin, 1996; 1–37.
2. Deming TJ. Polypeptide materials: new synthetic methods and applications. *Adv. Mater*. 1997; **9**: 299–311.
3. Tirrel JG, Fournier MJ, Mason TL, Tirell DA. Biomolecular materials. *Chem. Eng. News* 1994; **19**: 40–51.
4. Berg RH, Hvilsted S, Ramanujam PS. Peptide oligomers for holographic data storage. *Nature* 1996; **383**: 505–508.
5. Rasmussen PH, Ramanujam PS, Hvilsted S, Berg RH. Accelerated optical holographic recording using bis-DNO. *Tetrahedron Lett*. 1999; **40**: 5953–5956.
6. Rasmussen PH, Ramanujam PS, Hvilsted S, Berg RH. A remarkably efficient azobenzene peptide for holographic information storage. *J. Am. Chem. Soc*. 1999; **121**: 4738–4743.
7. Egholm M, Nielsen PE, Buchardt O, Berg RH. Recognition of guanine and adenine in DNA by cytosine and thymine containing peptide nucleic acids (PNA). *J. Am. Chem. Soc*. 1992; **114**: 9677–9678.
8. Egholm M, Buchardt O, Nielsen PE, Berg RH. Peptide nucleic acids (PNA). Oligonucleotide analogues with an achiral peptide backbone. *J. Am. Chem. Soc*. 1992; **114**: 1895–1897.
9. Nielsen PE, Egholm M, Berg RH, Buchardt O. Sequence-selective recognition of DNA by strand displacement with a thymine-substituted polyamide. *Science* 1991; **254**: 1497–1500.
10. Kleinman MH, Bohne C. Use of photophysical probes to study dynamic processes in supramolecular structures. In *Molecular and Supramolecular Photochemistry*, Ramamurthy V, Schanze KS (eds). Marcel Dekker: New York, 1997; 391–466.
11. Winnik FM. Photophysics of preassociated pyrenes in aqueous polymer solutions and in other organised media. *Chem. Rev*. 1993; **93**: 587–614.
12. Parker CA, Joyce TA. Determination of triplet formation efficiencies by the measurements of sensitized delayed fluorescence. *Trans. Faraday Soc*. 1966; **62**: 2785–2792.
13. Bright FV. A new fiber-optic-based multifrequency phase-modulation fluorometer. *Appl. Spectrosc*. 1988; **42**: 1531–1537.
14. De Schryver FC, Boens N, Put J. Excited state behaviour of some bichromic system. *Adv. Photochem*. 1977; **10**: 359–463.
15. Sisido M. Molecular to supramolecular design of synthetic polypeptides. *Prog. Polym. Sci*. 1992; **17**: 699–764.
16. Merrifield RB. Solid phase peptide synthesis. I. The synthesis of a tetrapeptide. *J. Am. Chem. Soc*. 1963; **85**: 2149–2154.
17. Merrifield B. Solid phase synthesis. *Science* 1986; **232**: 341–347.
18. HyperChem 4.0. *Release 4 for Windows Molecular Modelling Systems (4)*. Hypercube, Inc, 1994.
19. Dyke DAV, Pryor BA, Smith PG, Topp MR. Nanosecond time-resolved fluorescence spectroscopy in the physical chemistry laboratory: formation of the pyrene excimer in solution. *J. Chem. Educ*. 1998; **75**: 615–620.
20. Birks JB. *Excimers. Photophysics of Aromatic Molecules*. John Wiley & Sons Ltd: London, 1970; 301–371.
21. Birks JB. Excimers. *Rep. Prog. Phys*. 1975; **38**: 903–974.
22. Schweitzer D, Colpa JP, Behnke J, Hausser KH, Haenel M, Staab HA. Transannular interactions in [2.2] phanes as studied by magnetic resonance and optical spectra. *Chem. Phys*. 1975; **11**: 373–384.
23. Egusa S, Sisido M, Imanishi Y. One-dimensional aromatic crystals in solution. 4. Ground- and excited-state interactions of poly(L-1-pyrenylalanine) studied by chiroptical spectroscopy including circular polarized fluorescence and fluorescence-detected circular dichroism. *Macromolecules* 1985; **18**: 882–889.
24. Steinberg IZ. Circular polarization of luminescence: biochemical and biophysical applications. *Annu. Rev. Biophys. Bioeng*. 1978; **7**: 113–137.
25. Richardson FS, Riehl JP. Circularly polarized luminescence spectroscopy. *Chem. Rev*. 1977; **77**: 773–792.
26. Egusa S, Sisido M, Imanishi Y. Synthesis and spectroscopic properties of poly (L-1-pyrenylalanine), *Chem. Lett*. 1983; 1307–1310.
27. Inai Y, Sisido M, Imanishi Y. Strong circular polarization in the excimer emission from a pair of pyrenyl groups linked to a polypeptide chain. *J. Phys. Chem*. 1990; **94**: 2734–2735.
28. Inai Y, Sisido M, Imanishi Y. Excimer formation on a polypeptide carrying two pyrenyl groups in the middle of an α-helical main chain. *J. Phys. Chem*. 1990; **94**: 8365–8370.
29. Oishi O, Yamashita S, Ohno M, Lee S, Sugihara G, Nishino N. Peculiar photophysical properties of a conformationally proximal pyrene-pair. *Chem. Phys. Lett*. 1997; **269**: 530–534.
30. Goedeweeck R, De Schryver FC. Solvent effects on intramolecular excimer formation in *N*-acetyl-bis(pyrenylalanine)-methylester. *Photochem. Photobiol*. 1984; **39**: 515–520.

